Journal of Organometallic Chemistry 714 (2012) 32–40

Contents lists available at SciVerse ScienceDirect

Journal of Organometallic Chemistry

journal homepage: www.elsevier.com/locate/jorganchem

An NMR study on the reaction of substituted dimethyl zirconocenes with dimethylanilinium borate

Luca Rocchigiani, Gianfranco Bellachioma, Cristiano Zuccaccia, Alceo Macchioni*

Dipartimento di Chimica, Università degli Studi di Perugia, Via Elce di sotto 8, I-06123, Perugia, Italy

ARTICLE INFO

Article history:
Received 21 December 2011
Received in revised form
7 February 2012
Accepted 8 February 2012

Keywords:
Zirconocenes
NMR spectroscopy
Ion pairs
CH activation
Ring substituent effect

ABSTRACT

The reaction of a series of dimethyl zirconocenes [$Me_2Si(Cp)_2ZrMe_2$, **1**; $Cp^{t-bu}{}_2ZrMe_2$, **2**; $Cp^{n-bu}{}_2ZrMe_2$, **3**; Ind_2ZrMe_2, **4**; $Cp^{Me4}{}_2ZrMe_2$, **5**; $Cp^{*}{}_2ZrMe_2$, **6**] with $[HNMe_2Ph][B(C_6F_5)_4]$ was investigated by means of NMR spectroscopy. It was found that protonolysis of a Zr–Me group occurred generating a coordinative vacancy at the metal center and methane. Cations coming from **1**–**4** dimethyl precursors bound NMe_2Ph, liberated from the protonation process, and formed zirconaaziridinium ion pairs {$[Me_2Si(Cp)_2Zr(\eta^2-CH_2NMePh)][B(C_6F_5)_4]$, **7**; $[Cp^{t-bu}{}_2Zr(\eta^2-CH_2NMePh)][B(C_6F_5)_4]$, **8**; $[Cp^{n-bu}{}_2Zr(\eta^2-CH_2NMePh)][B(C_6F_5)_4]$, **9**; $[Ind_2Zr(\eta^2-CH_2NMePh)][B(C_6F_5)_4]$, **10**}, reasonably as a consequence of CH activation of one Me group of coordinated NMe_2Ph and methane elimination. The intramolecular/interionic structures and dynamics of **7**–**10** ion pairs were investigated by ^1H, ^{13}C and ^{19}F 1D-and 2D-NMR techniques. The reactions of **7** and **10** ion pairs with 2-methyl-1-heptene afforded stable diastereoisomeric ion pairs bearing a five-member azametallacycle.

1. Introduction

Many studies have been devoted to understanding the relationships between molecular structure and catalytic activity of group IV metallocenium catalysts for olefin polymerization [1–4]. Particularly, it has been shown that the nature of Cp-substituents can play a crucial role in tailoring the electronic and steric properties of catalysts leading to the possibility of finely controlling their activity and selectivity [5–8]. Cp-substituents not only exert their effect on all the steps involved in the polymerization process but they also modulate the ion pairing phenomenon between the cationic active species and its weakly coordinating counterion [9–12].

Ammonium salts $[HNR_3][X]$ are commonly used as activators for dialkyl precursors [13]; they act as Brönsted acids protonating an alkyl group, with the formation of the catalytically-active ion pairs, related alkane, and NR_3 (1).

$$L_nM(R')_2 + [HNR_3][X] \rightarrow [L_nM(R')][X] + R' - H + NR_3 \quad (1)$$

Very active catalytic ion pairs are generated when $[HNMe_2Ph][B(C_6F_5)_4]$ is used as activator due to the moderate basicity of NMe_2Ph [14] and weakly coordinating tendency of $B(C_6F_5)_4^-$. Even though the catalytic activity is not strongly affected by the presence of NMe_2Ph in solution, the latter is far from being considered an innocent species toward zirconocenes. As a matter of fact, evidence for coordination of NMe_2Ph at different metallocenium cations was reported [15,16]. Notably, Bochmann and co-workers isolated and fully characterized the adduct $[(IPCF)ZrMe(NMe_2Ph)][B(C_6F_5)_4]$ [IPCF = $Me_2C(C_5H_4)$(fluorenyl)] [17].

During our studies on the effect of the chain length on the self-aggregation tendency of zirconocenium ion pairs [18,19], we investigated the activation reaction of Cp_2ZrMe_2 with several $[HNMeRR'][B(C_6F_5)_4]$. In line with previous findings [20,21], we observed a quantitative coordination of the amine at the metal center and subsequent C–H activation of the NMe group leading to the formation of stable zirconaaziridinium ion pairs (Scheme 1) that were characterized in terms of interionic structure [18,19], intramolecular dynamics [22] and reactivity with olefins [23].

With the aim of evaluating the scope of such a reaction, we decided to explore the activation reaction of differently substituted zirconocenes $[Me_2Si(Cp)_2ZrMe_2$ (**1**), $Cp^{t-bu}{}_2ZrMe_2$ (**2**),$Cp^{n-bu}{}_2ZrMe_2$ (**3**), Ind_2ZrMe_2 (**4**), $Cp^{*}{}_2ZrMe_2$ (**5**), $Cp^{Me4}{}_2ZrMe_2$ (**6**), Scheme 2] with $[HNMe_2Ph][B(C_6F_5)_4]$. The results are reported herein. For systems that cleanly afforded the corresponding zirconaaziridinium ion pairs, the interionic structure and the dynamic behavior in solution were investigated by means of NOE NMR spectroscopy. Finally, the reactivity of substituted metallacycles with 2-methyl-1-heptene was explored.

* Corresponding author. Tel.: +39 075 5855579; fax: +39 075 5855598.
E-mail addresses: alceo@unipg.it, alceo.macchioni@gmail.com (A. Macchioni).

0022-328X/$ – see front matter © 2012 Elsevier B.V. All rights reserved.
doi:10.1016/j.jorganchem.2012.02.011

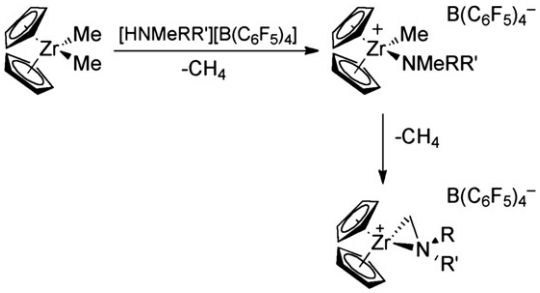

Scheme 1. Synthesis of zirconaaziridinium ion pairs.

2. Results and discussion

2.1. Reactivity of *1*–*6* with dimethylanilinium borate

The activation reaction of **1**–**6** precursors with 1 equivalent of $[HNMe_2Ph][B(C_6F_5)_4]$ in C_6D_6 led to an instantaneous evolution of CH_4, reasonably due to the protonolysis of one of the two ZrMe groups and the formation of the corresponding cationic species. The subsequent course of the reaction was dependent on the nature of the metallocenes as described in the following.

2.1.1. $Me_2Si(Cp)_2ZrMe_2$ (*1*)

An oil precipitated from the C_6D_6 solution and no trace of free NMe_2Ph was observed in the ^1H NMR spectrum of the supernatant. After some workup, the oily phase was dissolved in C_6D_5Cl and the ^1H NMR spectrum revealed the presence of two sets of signals. In strict analogy with the results obtained for Cp_2ZrMe_2 [19], the most intense resonances were due to the complex $[Me_2Si(Cp)_2ZrMe(NMe_2Ph)][B(C_6F_5)_4]$ while the other set of signals were compatible with the formation of the ion pair $[Me_2Si(Cp)_2Zr(\eta^2-CH_2NMePh)][B(C_6F_5)_4]$ (**7**) bearing the three-member heterocycle (Scheme 1). Over the course of several hours, the selective C–H activation of one of the NMe groups and methane elimination proceeded, leading to the complete formation of **7** (Scheme 1).

Ion pair **7** was characterized by crossing the information coming from 1D- and 2D- homo- and heteronuclear NMR experiments. The starting point was the resonance at $\delta_H = 2.43$ ppm, which was assigned to the NMe group. Such NMe moiety displayed a strong NOE interaction with the doublet at $\delta_H = 2.13$ ppm which was assigned to $ZrCH_2^u$ (see Scheme 3 for labeling of proton and carbon atoms). The latter resonance showed strong dipolar contacts with the two multiplets at $\delta_H = 6.03$ and $\delta_H = 5.36$ ppm that were due to $H2^u$ and $H1^u$ (Fig. 1). These two resonances were distinguished on the basis of the strong NOE of $H1^u$ with the singlet at $\delta_H = 0.09$ ppm that was, in turn, assigned to the methyl group of the silicon bridge labeled as $SiMe^C$ (Fig. 1). From $H2^u$, the resonances of $H3^u$ and $H4^u$ were easily located at $\delta_H = 5.65$ and $\delta_H = 5.08$ ppm, respectively, by following the scalar connectivity in the ^1H COSY NMR spectrum (Fig. 2). $SiMe^N$ resonance was identified since it showed a selective NOE with $H4^u$. The resonances of the four Cp^d protons were assigned similarly starting from the resonance of $ZrCH_2^q$. The assignment of all the carbon resonances was easily achieved by performing ^1H, ^{13}C HMBC and HMQC NMR experiment and allowed to confirm the hypothesized structure of **7**.

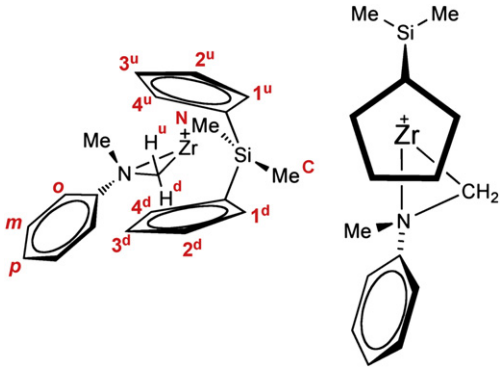

Scheme 3. Structure and numbering of **7**.

2.1.2. $Cp^{t-bu}{}_2ZrMe_2$ (*2*)

The reaction of NMe_2Ph with $Cp^{t-bu}{}_2ZrMe^+$ occurred similarly to that described above for **1** (Scheme 1). The ^1H NMR spectrum of the final product showed the presence of two doublets having a scalar coupling constant of 8.7 Hz at $\delta_H = 3.91$ and $\delta_H = 2.78$ ppm. This pattern of resonances was associated with the presence of a $ZrCH_2$ moiety and indicated that, also in this case, the coordination of dimethylaniline was followed by the C–H activation that afforded the corresponding ion pair $[Cp^{t-bu}{}_2Zr(\eta^2-CH_2NMePh)][B(C_6F_5)_4]$ (**8**). The ^1H NMR spectrum of the reaction mixture contained some residual resonances of $[Cp^{t-bu}{}_2ZrMe(NMe_2Ph)][B(C_6F_5)_4]$ (Supporting Information) after 12 h at 305 K. As seen above, the formation of the three-member heterocycle made the two Cp rings magnetically not equivalent. This resulted in the presence of eight separated resonances for the Cp-hydrogen atoms and two distinct signals for the protons of the two t-butyl groups in

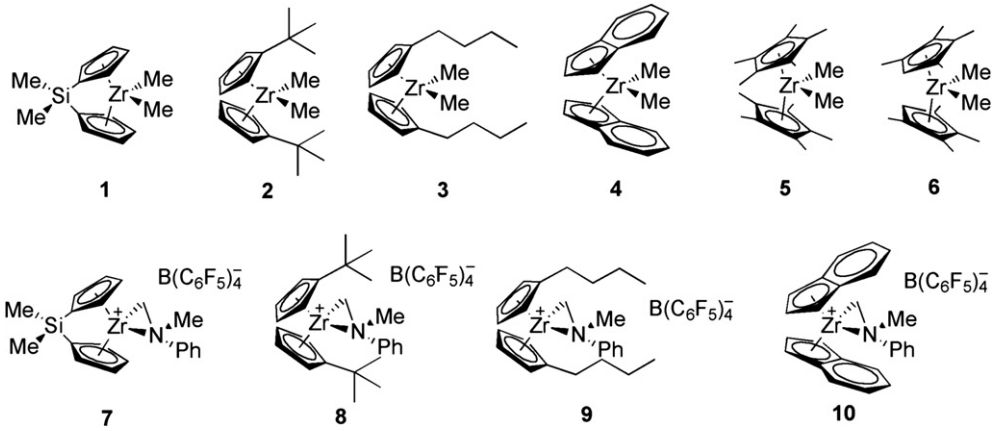

Scheme 2. Sketch of **1**–**6** dimethyl precursors and **7**–**10** ion pairs.

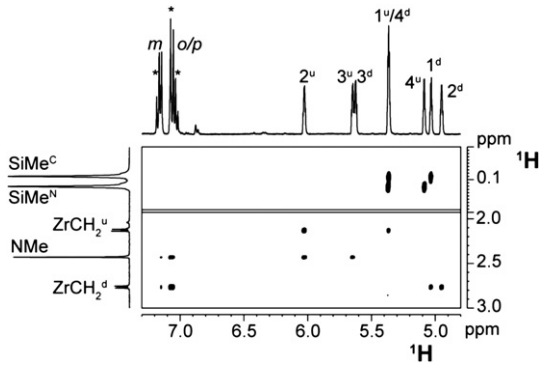

Fig. 1. A section of ^{1}H NOESY NMR spectrum of **7** recorded in C_6D_5Cl at 297 K. Asterisks denote the resonances of solvent.

the ^{1}H NMR spectrum (Supporting Information). Assignment of proton and carbon resonances was carried out starting from the strong NOE contact between the singlet at $\delta_H = 2.86$ ppm and the doublet at $\delta_H = 2.78$ ppm which were due to NMe and $ZrCH_2^u$, respectively (see Scheme 4 for numbering).

As can be seen from the section of ^{1}H NOESY NMR spectrum reported in Fig. 3, a selective dipolar contact was present between $ZrCH_2^d$ group ($\delta_H = 3.91$ ppm) and the singlet at $\delta_H = 0.81$ ppm which was assigned to the t-butyl group of the Cp ring in down position (t-Bu^d). The resonance of the quaternary carbon atom C5^d ($\delta_C = 143.1$ ppm) was identified from its long-range scalar correlation with t-Bu^d in the ^{1}H, ^{13}C HMBC NMR spectrum (Fig. 4). From the same spectrum, the resonances of hydrogen atoms belonging to the same Cp ring were found at $\delta_H = 6.21$, 5.73, 5.66 and 5.04 ppm by virtue of their long-range couplings with C5^d (Fig. 4). These signals were distinguished following the pattern of dipolar interactions: the signal at $\delta_H = 5.66$ ppm displayed NOE contact with both $ZrCH_2^d$ and t-Bu^d and it was assigned to H1^d, while the resonance at $\delta_H = 5.73$ ppm showed only a dipolar interaction with t-Bu^d and was labeled as H4^d. Finally, H2^d and H3^d were responsible for the resonances at $\delta_H = 5.04$ and $\delta_H = 6.21$ ppm, respectively, based on their selective NOE interaction with H1^d and H4^d (Fig. 5a). Using the same strategy, the proton resonances of the other Cp ring located at $\delta_H = 6.77$, 6.33, 6.04 and 5.39 ppm were assigned starting from the proton signal of t-Bu^u at $\delta_H = 0.87$ ppm. The signal at $\delta_H = 6.04$ ppm showed dipolar contacts both with NMe and t-Bu^u

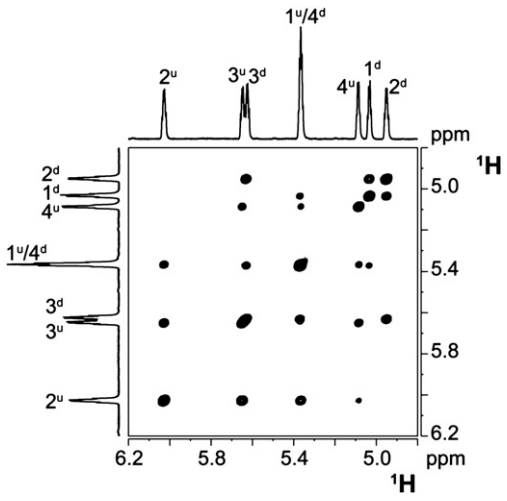

Fig. 2. A section of ^{1}H COSY NMR spectrum of **7** recorded in C_6D_5Cl at 297 K.

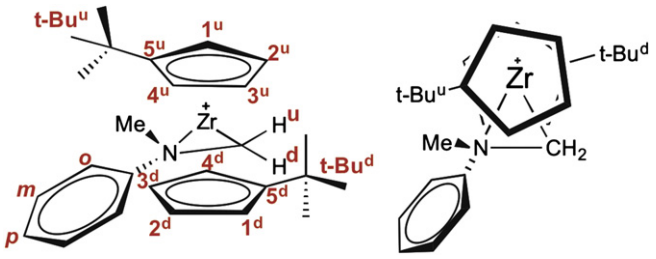

Scheme 4. Structure and numbering of **8**.

and it was assigned to H1^u (Fig. 5a), while the one at $\delta_H = 6.77$ ppm interacted with $ZrCH_2^u$ and was assigned to H2^u. H3^u and H4^u were discriminated since only the signal at $\delta_H = 6.33$ ppm interacted with t-Bu^u, so it was identified as H4^u. All the carbon resonances were easily assigned following one-bond and multiple-bonds proton-carbon scalar correlations in ^{1}H, ^{13}C HMQC and ^{1}H, ^{13}C HMBC NMR spectra, respectively.

The observation of selective inter-rings NOE interactions allowed the relative orientation of the two Cp rings in solution to be disclosed. Dipolar contacts were observed for the pairs H3^u/t-Bu^d and H3^d/t-Bu^u (Fig. 5a), H4^d/H3^u and H4^u/H4^d (Fig. 5b) suggesting that a staggered conformation (Scheme 4) was predominant in solution. Since dipolar interactions between t-Bu^u and $ZrCH_2^u$ were not observed, we concluded that the Cp in up position oriented the t-butyl group far away from the methylenic moiety and close to the NMe. On the contrary, the Cp on the bottom pointed the t-butyl close to the $ZrCH_2$ as indicated by the strong NOE between $ZrCH_2^d$ and t-Bu^d.

2.1.3. $Cp^{n-bu}{}_2ZrMe_2$ (**3**)

The reaction of **3** with dimethylanilinium borate afforded the ion pair **9** bearing the three-member azametallacycle in 3 h. This was deduced by the observation, in the ^{1}H NMR spectrum (Supporting Information), of a resonance at $\delta_H = 2.51$ ppm, that was assigned to the NMe group, and two doublets at $\delta_H = 2.87$ and $\delta_H = 2.22$ ppm ($J_{H,H} = 8.4$ Hz), clearly indicating the formation of an heterocyclic CH_2 moiety. Unfortunately, **9** decomposed in a few hours preventing the possibility to acquire 2D-NMR spectra and perform a full assignment of resonances.

2.1.4. Ind_2ZrMe_2 (**4**)

The reaction between **4** and dimethylanilinium borate afforded the zirconaaziridinium ion pair **10** after 12 h at 308 K in a 80% yield (based on NMR integration). The C–H activation was proved by the formation of CH_4 and the appearance of two doublets at $\delta_H = 0.52$ and $\delta_H = -0.19$ ppm in the ^{1}H NMR spectrum, due to the diastereotopic protons of the $ZrCH_2$ moiety. The aromatic region of the spectrum was rather complex (Supporting Information) and the full assignment of resonances was not achieved also due to the further

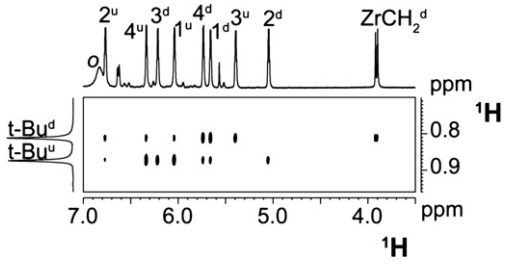

Fig. 3. A section of ^{1}H NOESY NMR spectrum of **8** recorded at 297 K in C_6D_5Cl.

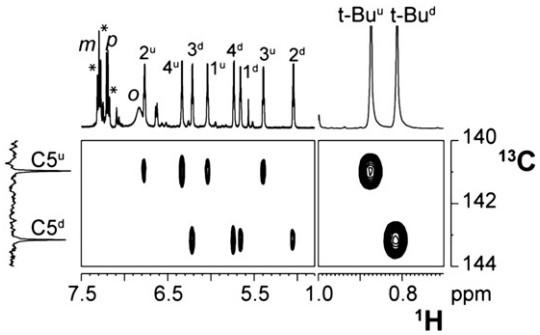

Fig. 4. A section of ^{1}H, ^{13}C HMBC NMR spectrum of **8** recorded at 297 K in C_6D_5Cl. Asterisks denote the resonances of solvent.

complication introduced by the presence of extensive chemical exchange in the ^{1}H NOESY NMR spectrum (Fig. 6). For example, both protons of the $ZrCH_2$ showed apparent dipolar interactions with the singlet at $\delta_H = 2.36$ ppm that was the NMe group. Fortunately, the exchange process was not fast enough to completely delete the selectivity and it was observed that the NOE interaction between NMe and the resonance at $\delta_H = 0.52$ ppm was stronger (Fig. 7). Consequently, we assigned the latter signal to $ZrCH_2^u$ (Scheme 5). Likewise, the signal at $\delta_H = 5.65$ ppm was assigned to H1^u, due to its stronger NOE correlation with NMe. Starting from H1^u, resonances of H2^u ($\delta_H = 6.02$ ppm) and H3^u ($\delta_H = 6.19$ ppm) were easily located following the pattern of scalar connectivity in the ^{1}H COSY NMR spectrum (Supporting Information). The resonance at $\delta_H = 5.45$ ppm was assigned to H1^d since it showed a strong correlation with the doublet at $\delta_H = 6.97$ ppm, which was due to the *ortho*-protons of the phenyl ring on the nitrogen atom. Having assigned H1^d, H2^d ($\delta_H = 5.96$ ppm) and H3^d ($\delta_H = 5.86$ ppm) resonances were identified by analyzing the ^{1}H COSY NMR spectrum as the same of the other ring (Supporting Information). Unfortunately, the protons of the annulated phenyl rings of the indenyl groups could not be safely assigned since a discrimination

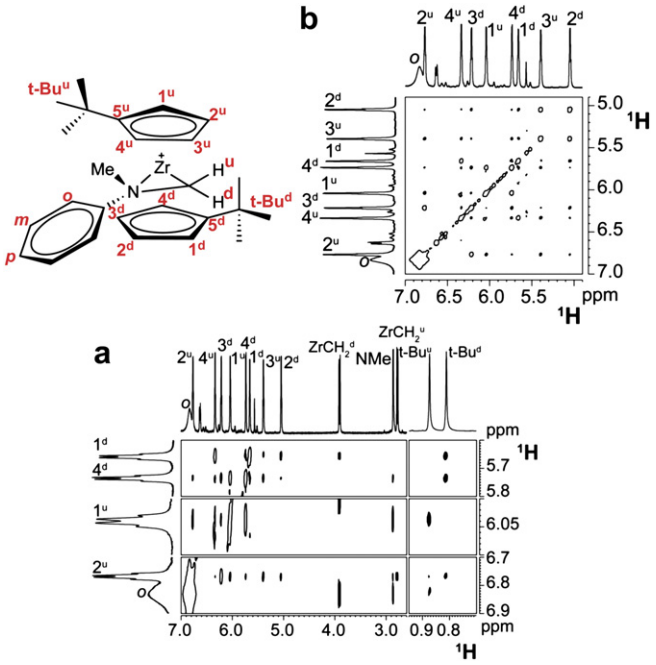

Fig. 5. Sections of ^{1}H NOESY NMR spectrum of **8** recorded at 297 K in C_6D_5Cl.

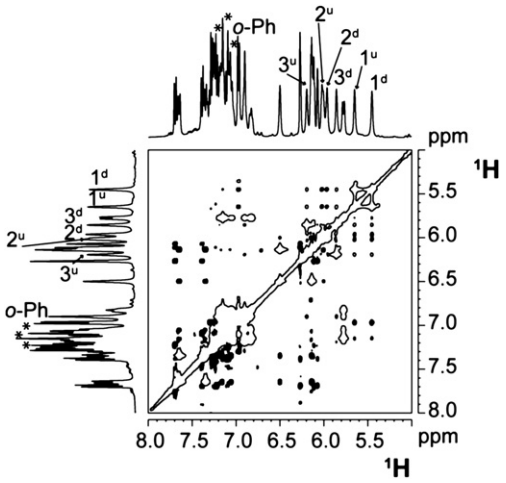

Fig. 6. A section of ^{1}H NOESY NMR spectrum of **10** recorded at 297 K in C_6D_5Cl. Asterisks denote the resonances of solvent.

between genuine NOE cross peaks and apparent dipolar interactions due to chemical exchange was not possible.

2.1.5. $Cp^*_2ZrMe_2$ (**5**)

The reaction of **5** with dimethylanilinium borate proceeded differently from the cases discussed above. After mixing the reagents in C_6D_6, a vigorous gas evolution and the formation of an oily phase were observed, in accordance with the protonolysis of one methyl group of the precursor. The ^{1}H NMR spectrum of the C_6D_6 solution showed the presence of a large excess of free dimethylaniline together with a Cp* resonance at $\delta_H = 1.34$ ppm and a signal at $\delta_H = 0.51$ ppm likely due to a ZrMe group. The evolution of the mixture was monitored by NMR over a period of 1 h. As can be seen from Fig. 8, the intensity of both resonances decreased and the formation of CH_4 ($\delta_H = 0.15$ ppm) and CH_3D (triplet at $\delta_H = 0.14$ ppm) was observed. Importantly, there was no evidence neither for dimethylaniline coordination nor for the formation of the three-member heterocycle. The production of partially deuterated methane was a clear indication of a C–D activation of the C_6D_6 molecule. Similar reactions were observed by Jordan et al. when C_6D_5Cl was used as a solvent [24,25].

2.1.6. $Cp^{Me4}_2ZrMe_2$ (**6**)

The reaction of **6** with dimethylanilinium borate formed a large amount of CH_4, indicating also in this case the protonolysis of one ZrMe group occurred (Supporting Information). This gas evolution was accompanied by the separation of an oily phase at the bottom

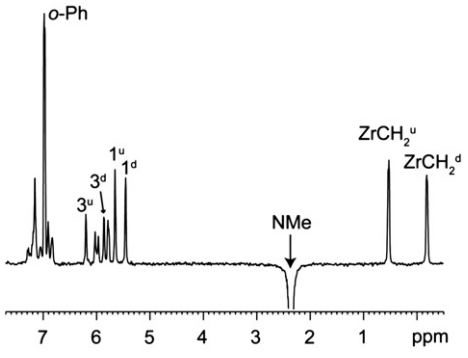

Fig. 7. F2 trace (direct dimension) of ^{1}H NOESY NMR spectrum recorded in C_6D_5Cl at 297 K showing the selective dipolar contacts of NMe in **10**.

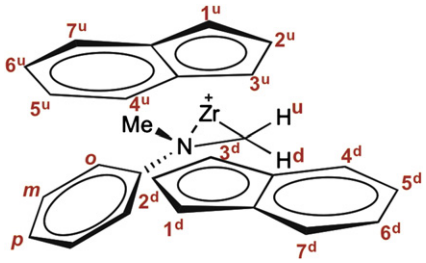

Scheme 5. Structure and numbering of **10**.

of the NMR tube and, as observed for **5**, there was no evidence for the coordination of the amine. The ^{1}H NMR spectrum of the oil in C_6D_5Cl was complex (Supporting Information) and it was not possible to identify any of the products present in the mixture.

Summarizing, it appears that cations generated from **1**–**4** precursors are capable of coordinating and activating NMe_2Ph while cations from **5** and **6** are not. Such a different behavior is likely due to a combination of steric and electronic effects since **1**–**4** are not only less encumbered than **5**–**6** [26] but they also bear most acidic metal centers [27]. Once the Zr–N bond is formed, the C–H activation of one of the NMe groups of the amine leads to the formation of the zirconaziridinium structures **7**–**10**.

The reaction time required to obtain **7**, **8** and **10** ion pairs is considerably longer with respect to that of the unsubstituted cation $[Cp_2ZrMe(NMe_2Ph)]$ [19]. Assuming that the C–H activation proceeds by an agostic interaction between the metal and the NMe group, it could be speculated that in the case of **1**, where a more electron density on the metal is expected [28], the tendency to react is lower. On the contrary, for the more electron deficient **2** and **4** complexes [31], it is reasonable to believe that the steric encumbrance of the ligand slows down the reorientation of the NPh group that is mandatory for the formation of the constrained heterocycle.

2.2. Interionic structure

The interionic structure (i.e. the relative cation–anion orientation) of **7**, **8** and **10** ion pairs was investigated in C_6D_5Cl by means of ^{19}F,^{1}H HOESY NMR experiments [29–36]. The ^{19}F,^{1}H HOESY NMR spectrum of **7** (Fig. 9) showed that interionic dipolar contacts involving *m*-F were slightly stronger than those due to *o*-F, as usually observed for ion pairs bearing the $B(C_6F_5)_4^-$ anion [37].

It was evident that all the protons belonging to the cation were dipolarly coupled with the fluorine atoms of the anion and this suggested a low selectivity in the ion pairing. However, an accurate

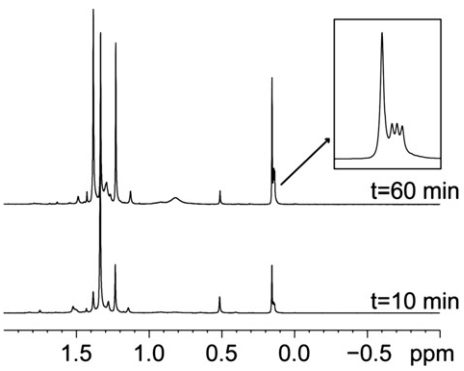

Fig. 8. Evolution of the ^{1}H NMR spectrum for the reaction between **5** and $[HNMe_2Ph][B(C_6F_5)_4]$ in C_6D_6 at 297 K.

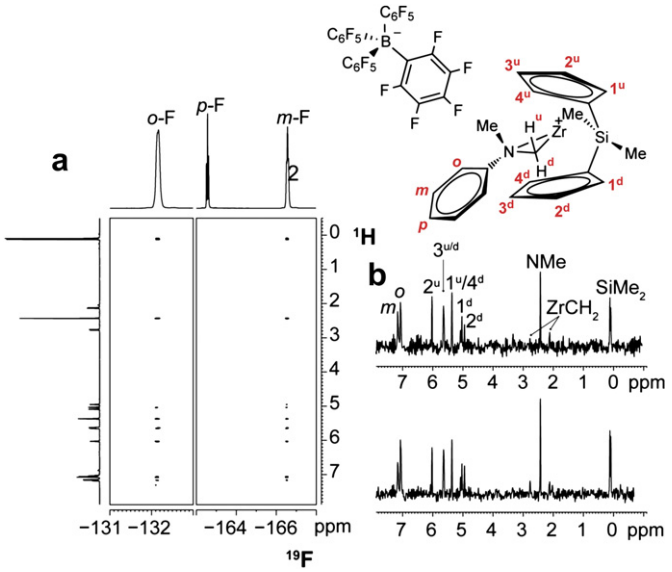

Fig. 9. a) ^{19}F, ^{1}H HOESY NMR spectrum of **7** recorded in C_6D_5Cl at 297 K; b) Two F1 traces (indirect dimension) relative to *o*-F (top) and *m*-F (bottom).

integration of the signals showed that the strongest heteronuclear dipolar interactions were present between *o*-F/*m*-F and $H2^u$, $H3^u$/$H3^d$ and $H1^u$/$H4^d$ pairs, NMe, *ortho* and *meta* protons of the phenyl ring bound to the nitrogen and the two methyl groups bound to the silicon. By combining this pattern of dipolar interactions, it was deduced that the anion locates close to the NMePh moiety and shifted toward the Cp^u, as indicated by the difference in the relative intensity of the contacts between $H2^d$ and $H2^u$ (Fig. 9).

In the case of **8**, the ^{19}F, ^{1}H HOESY NMR spectrum recorded in C_6D_5Cl (Fig. 10) showed strong dipolar contacts of the fluorine atoms of the anion with the hydrogen atoms of the NMe group and both the tert-butyls of the cation. Interestingly, the interactions with the other protons were much weaker and in some cases undetectable. This suggested that the steric bulk provided by the t-Bu groups forced the anion further away from the cation.

No selective dipolar contacts were observed for **9**, where the anion shows NOEs with almost all the cationic protons, except those belonging to the $ZrCH_2$ moiety (Supporting Information).

2.3. Intramolecular dynamics

In the ^{1}H NOESY NMR spectra of **8** and **10** ion pairs several exchange cross peaks were observed, indicating the presence of dynamic processes. In particular, exchange cross peaks were observed between the two hydrogen atoms of the $ZrCH_2$ moiety and the two t-butyl substituents for **8**. In addition, in the Cp-region

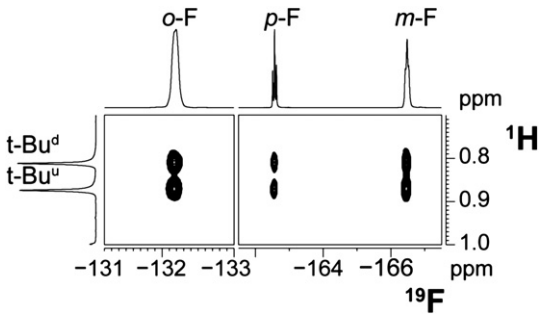

Fig. 10. A section of the ^{19}F,^{1}H HOESY NMR spectrum of **8** recorded in C_6D_5Cl at 297 K.

of the spectrum, a selective pattern of exchanges was identified (Fig. 5b): $H2^d$ with $H3^u$, $H2^u$ with $H3^d$, $H1^u$ with $H4^u$ and $H4^d$, $H1^d$ with $H4^u$ and $H4^d$. A rational explanation of such fluxional behavior can be achieved considering the lability of the Zr–N interaction and the possibility for Cp groups to rotate [38,22]. In fact, up-down exchanges may be caused by the broken of the Zr–N bond, pyramidal inversion and re-coordination of the chiral N-atom (PI, Scheme 6). While back-in front exchanges of Cp protons may derive from a readjustment of the Cp-configuration aimed at minimizing the steric Ph/t-butyl interactions (Scheme 6). Finally, since the intensity of exchange cross peaks between Cp and t-butyl protons is higher than that of the $ZrCH_2$ protons it has to be hypothesized that a back-skip (BS) process, which exchanges only the former protons leaving the latter unaffected, is operative (Scheme 6).

Despite the full assignment of resonances for **10** was not possible, an inspection of the exchange cross peaks of H1, H2 and H3 (Fig. 6) was sufficient to establish that the pattern of chemical exchange was similar to that of **8**. For example, $H1^u$ showed chemical exchange with $H1^d$, $H3^u$ with $H3^d$, and $H2^u$ with $H2^d$. Also in this case, the signals corresponding to the two hydrogen atoms of the $ZrCH_2$ moiety were in mutual exchange. These observations suggested that the exchange mechanism described in Scheme 6 was operative also for **10**. In contrast, exchange cross peaks were not observed in the ^{1}H NOESY spectrum of **7**.

By a semi-quantitative integration of the exchange cross peaks in the spectra of **8** and **10**, it was found that rates of the exchange processes are higher in the latter. Therefore, the scale of exchange rate is **10** > **8**>**7**. This trend in the dynamic behavior seems to correlate with steric effects, since the rate of the fluxional processes increased with the steric encumbrance of the ligand on the front side of the molecule. For **7** there are no bulky groups pointing towards the nitrogen and this could lead to a better arrangement of the heteroycle and a slower dinamicity. In the case of **8** and **10**, the bulky groups pushes on the NPh moiety and this could decrease the stability of the Zr–N bond; this effect seems to be higher in the case of the bis-indenyl species.

2.4. Reaction of *7*, *8* and *10* ion pairs with 2-methyl-1-heptene

Zirconaaziridinium ion pairs **7**, **8** and **10** were reacted with 2-methyl-1-heptene in C_6D_5Cl. In the case of **7** a fast reaction took place that did not go to completion (Supporting Information). An inspection of the ^{1}H NMR spectrum allowed identifying four new doublets in the 2.5–3.0 region and other four doublets between 2.0 and 0.5 ppm that had almost the same intensity. These spectral features suggested that a 1,2 single-insertion of 2-methyl-1-heptene into the Zr–C bond of the heterocycle occurred, resulting in the formation of an equimolar mixture of two diastereoisomeric azametallapentacycles **11** differing in the relative configuration of the nitrogen and carbon stereogenic centers (RR/SS or RS/SR, Scheme 7).

The ^{1}H NMR spectrum of the reaction mixture (Supporting Information) was very complicated, since it contained resonances of the excess of heptene and residual **7** that were partially overlapped to those belonging to **11**(RR/SS) and **11**(RS/SR). This did not allowed to perform a full assignment of resonances. Nevertheless, important structural information was obtained from the ^{1}H NOESY NMR spectrum (Fig. 11). For example, a strong NOE interaction between the NMe resonance at δ_H = 2.64 ppm and the CMe at δ_H = 1.14 ppm was observed indicating that these two resonances are due to the **11**(RR/SS) diastereoisomer. Starting from these resonances, the entire skeleton of the RR/SS five-member heterocycle was assigned: the selective NOE between the NMe at δ_H = 2.64 ppm and the doublet at δ_H = 2.38 ppm allowed to label the latter as NCH_2^u while the strong dipolar interaction of the CMe at δ_H = 1.14 ppm with the doublet at δ_H = 1.62 ppm assigned that signal to $ZrCH_2^u$. The resonances of NCH_2^d (δ_H = 3.06 ppm) and $ZrCH_2^d$ (δ_H = 0.94 ppm) were identified by ^{1}H COSY NMR spectrum (Supporting Information). The assignment of the doublets belonging to **11**(RS/SR) isomer was performed analogously.

No reaction was observed when 2-methyl-1-heptene was reacted with **8**, likely due to the steric hindrance of the t-Bu substituents that inhibited olefin coordination. On the contrary, **10** reacted with 10 equivalents of 2-methyl-1-heptene affording two diastereoisomeric five-member heterocycles. Due to the complexity of the ^{1}H NMR spectrum, the full resonance assignment was not possible but crucial structural information was obtained by ^{1}H NOESY NMR spectroscopy (Supporting Information). For example the strong dipolar contact between the NMe group and a CMe moiety allowed identifying the RR/SS isomer, while the interaction of the other NMe with a CCH_2 group accounted for the formation of the RS/SR isomer.

3. Conclusions

We have herein shown that only least encumbered and least electron rich **1**–**4** dimethyl zirconocenes react with $[HNMe_2Ph][B(C_6F_5)_4]$ leading to zirconaaziridinium ion pairs **7**–**10** by

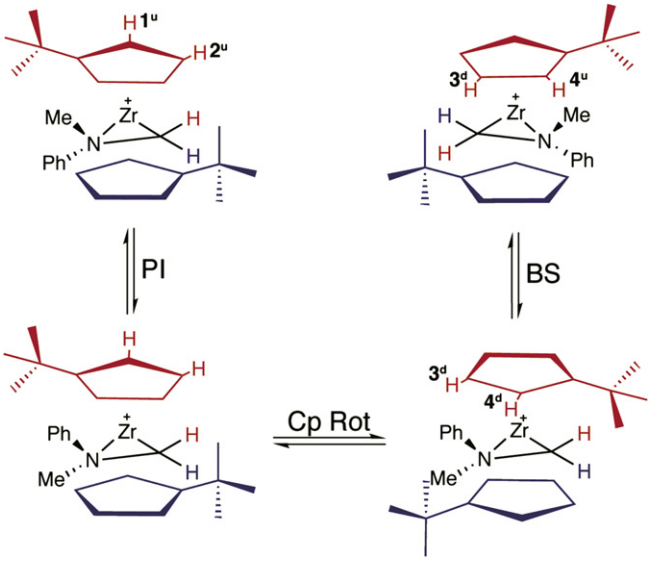

Scheme 6. Proposed mechanism for the fluxionality of **8**.

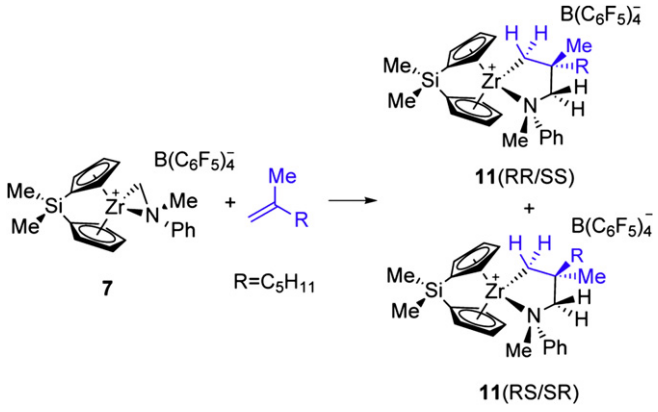

Scheme 7. Monoinsertion of 2-methyl-1-heptene into the Zr–C bond of **7**.

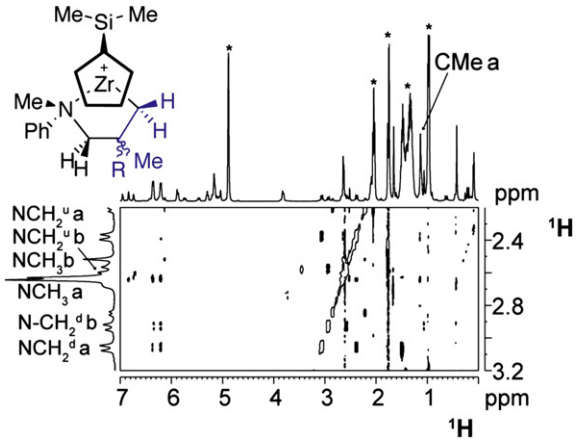

Fig. 11. A section of ^{1}H NOESY NMR spectrum of **11**(RR/SS and SR/RS) recorded in C_6D_5Cl at 297 K. Asterisks denote resonances of unreacted 2-methyl-1-heptene while labels "a" and "b" denote RR/SS and RS/SR diastereoisomers, respectively.

protonation of both the ZrMe groups caused by N–H and NCH_2–H activations of $HNMe_2Ph^+$ and Zr–NMe_2Ph, respectively. The Zr–N bond is rather labile in **7**–**10** ion pairs as demonstrated by the fact that they undergo a complex dynamic process involving the dissociation of the Zr–N bond, pyramidal inversion of the chiral N-atom, back-skip of the Zr–CH_2N(Me)Ph chain and final adjustment of substituted Cp rings in a conformation of minimum energy. The Zr–N labile bond is likely the key to obtain the diastereoisomeric ion pairs, having a five-member azametallacycle, from a single 1,2-insertion of 2-methyl-1-heptene into the Zr–C bond of zirconaaziridinium ion pairs.

4. Experimental section

4.1. General Procedures

All manipulations of air-sensitive materials were performed in flamed Schlenk glassware on a Schlenk line, interfaced to a diffusive high vacuum pump (10^{-5} mmHg), or in a nitrogen filled glovebox with an high capacity recirculator (<1 ppm O_2 and H_2O). All solvents were preventively distilled from Na, freeze-pump-thaw degassed on the high vacuum line, dried over Na/K alloy and vacuum transferred in storage Schlenk flasks with a PTFE valve. Deuterated solvents were freeze-pump-thaw degassed on the high vacuum line, dried over Na/K alloy (C_6D_6 and $CD_3C_6D_5$) or CaH_2 (C_6D_5Cl) and vacuum transferred in storage Schlenk flasks with a PTFE valve. Zirconocenium dichlorides $Me_2Si(Cp)_2ZrCl_2$, $Cp^{t-bu}{}_2ZrCl_2$, $Cp^{n-bu}{}_2ZrCl_2$, Ind_2ZrCl_2, $Cp^*{}_2ZrCl_2$ and $Cp^{Me4}{}_2ZrCl_2$ were purchased from Strem Chemicals. LiMe (1.66 M solution in ether) was obtained from Aldrich. N,N-dimethylanilinium tetrakis-pentafluorophenylborate was purchased from Boulder Sci. and used without further purifications. 2-methyl-1-heptene was purchased from Aldrich and freeze-pump-thaw degassed on the high vacuum line, dried over CaH_2 and distilled in a storage Schlenk flask with a PTFE valve.

One and two-dimensional ^{1}H, ^{13}C and ^{19}F NMR spectra were measured on a Bruker DRX 400 spectrometer and referencing is relative to TMS (^{1}H and ^{13}C) and CCl_3F (^{19}F). ^{1}H NOESY NMR [39] experiments were acquired by the standard three-pulse sequence or by the PFG version [40]. Two-dimensional ^{19}F,^{1}H HOESY NMR spectra were recorded by using the standard four-pulse sequence or its modified version [41]. The number of transients and data points were chosen according to the sample concentration and desired final digital resolution. Qualitative or semi-quantitative two-dimensional Overhauser spectra were recorded by using 1s relaxation delay and a mixing time comprised between 400 and 800 ms. NMR samples were prepared into the glovebox in J-Young NMR tubes by dissolving the suitable amount of compound in 0.6 ml of deuterated solvent.

4.2. Preparation of *1*–*6* dimethyl precursors and NMR data

The synthesis of the dimethyl derivatives was performed starting from the corresponding dichlorides by following the literature procedure described by Samuel and Rausch [42]. In a 50 ml reaction flask, connected with a J-Young valve to the high vacuum line, 1.0 g of dichloride precursor was charged and dissolved in approximately 30 ml of dry diethyl-ether. This suspension was cooled at −40 °C and 1.5 equivalents of LiMe (1.66 M solution in diethyl-ether) were added dropwise with a syringe in a period of 30 min. The temperature was maintained around −40 °C for 30 min and then was allowed to raise to 0 °C. After 10 min, the solvent was removed in vacuo and the reaction mixture was dried for 30 min. The reaction product was purified by vacuum sublimation and collected into the glovebox. All the reaction yields were between 30 and 60%.

1: ^{1}H NMR (C_6D_6, 297 K, 400.13 MHz) δ = 6.73 (m, 4H), 5.47 (m, 4H), 0.18 (s, 6H), 0.03 ppm (s, 6H). **2**: ^{1}H NMR (C_6D_6, 297 K, 400.13 MHz) δ = 5.82 (s, 4H), 5.78 (s, 4H), 1.81 (s, 18H), 0.02 ppm (s, 6H). **3**: ^{1}H NMR (C_6D_6, 297 K, 400.13 MHz) δ = 5.73 (pst, 4H, $^3J_{H,H}$ = 2.5 Hz), 5.53 (pst, 4H, $^3J_{H,H}$ = 2.5 Hz), 2.41 (m, 4H), 1.51 (m, 4H), 1.32 (m, 4H), 0.88 (t, 6H, $^3J_{H,H}$ = 7.3 Hz), −0.10 ppm (s, 6H). **4**: ^{1}H NMR ($CD_3C_6D_5$, 297 K, 400.13 MHz) δ = 7.18 (dd, 4H, $^3J_{H,H}$ = 6.5 Hz, $^3J_{H,H}$ = 3.1 Hz), 6.87 (dd, 4H, $^3J_{H,H}$ = 6.5 Hz, $^3J_{H,H}$ = 3.1 Hz), 5.77 (d, 4H, $^3J_{H,H}$ = 3.4 Hz), 5.61 (d, 4H, $^3J_{H,H}$ = 3.4 Hz), −0.86 ppm (s, 6H). ^{13}C{^{1}H} NMR ($CD_3C_6D_5$, 297 K, 100.55 MHz) δ = 137.1 (s), 124.6 (s), 124.0 (s), 114.5 (s), 99.4 (s), 35.3 ppm (s). **5**: ^{1}H NMR (C_6D_6, 297 K, 400.13 MHz) δ = 1.78 (s, 30H), −0.55 ppm (s, 6H). **6**: ^{1}H NMR (C_6D_6, 297 K, 400.13 MHz) δ = 4.74 (s, 2H), 1.95 (s, 24H), −0.53 ppm (s, 6H).

4.3. In situ generation of *7*–*10* ion pairs and NMR data

A suitable amount of the precatalyst and 1 equivalent of solid $[HNMe_2Ph][B(C_6F_5)_4]$ were loaded into a J-Young NMR tube and dissolved in approximately 0.6 ml of C_6D_6 at 298 K. Immediately, a vigorous gas evolution was observed and a red oily phase quickly settled to the bottom of the J-Young NMR tube. The supernatant solution was removed, the resultant oil was rinsed with benzene (2 × 1 ml) and dissolved in approximately 0.6 ml of C_6D_5Cl. The formation of the reaction product was followed by NMR as described in the Results and Discussion section and went to the completion in about 12 h at 305–310 K.

4.3.1. $[Me_2Si(Cp)_2ZrMe(NMe_2Ph)][B(C_6F_5)_4]$

^{1}H NMR (C_6D_5Cl, 297 K, 400.13 MHz) δ = 7.16 (m, buried with **7**), 7.06 (m, buried with **7**), 6.55 (d, 2H, $^3J_{H,H}$ = 7.9 Hz), 6.29 (m, 2H), 5.61 (m, 2H), 5.45 (m, 2H), 5.31 (m, 2H), 2.22 (s, 6H), 0.50 (s, 3H), 0.36 (s, 3H), 0.08 ppm (s, 3H).

4.3.2. $[Me_2Si(Cp)_2Zr(\eta^2\text{-}CH_2NMePh)][B(C_6F_5)_4]$ (*7*)

^{1}H NMR (C_6D_5Cl, 297 K, 400.13 MHz) δ = 7.16 (m, 2H, *meta*-H), 7.07 (d, 2H, *ortho*-H, $^3J_{H,H}$ = 8.0 Hz), 7.03 (t, 1H, *para*-H, $^3J_{H,H}$ = 7.5 Hz), 6.03 (m, 1H, $H2^u$), 5.65 (m, 1H, $H3^u$), 5.36 (m, 2H, $H1^u$+$H4^d$), 5.08 (m, 1H, $H4^u$), 5.03 (m, 1H, $H1^d$), 4.95 (m, 1H, $H2^d$), 2.76 (d, 1H, $ZrCH_2^d$, $^2J_{H,H}$ = 8.1 Hz), 2.43 (s, NMe), 2.13 (d, 1H, $ZrCH_2^u$, $^2J_{H,H}$ = 8.1 Hz), 0.12 (s, 3H, $SiMe^N$), 0.09 ppm (s, 3H, $SiMe^C$). ^{13}C{^{1}H} NMR (C_6D_5Cl, 297 K, 100.55 MHz) δ = 155.4 (s, *ipso*-C), 130.0 (s, *meta*-C), 128.0 (s, *para*-C), 125.8 (s, $C2^d$), 125.6 (s, $C2^u$), 122.1 (s, *ortho*-C), 120.5 (s, $C3^u$), 120.1 (s, $C3^d$), 110.9 (s, $C1^d$), 108.6 (s, $C1^u$),

107.7 (s, $C5^d$), 107.1 (s, $C4^d$), 104.6 (s, $C2^d$), 103.8 (s, $C5^u$), 57.3 (s, NMe), 54.9 (s, $ZrCH_2$), −6.7 (s, $SiMe^N$), −7.2 ppm (s, $SiMe^R$). ^{19}F NMR (C_6D_5Cl, 297 K, 376.65 MHz) δ = −132.1 (brd, *ortho*-F), −162.6 (t, *para*-F, $^3J_{F,F}$ = 21.3 Hz), −166.6 ppm (m, *meta*-F).

4.3.3. [(Cp^{t-bu})$_2$ZrMe(NMe$_2$Ph)][B(C_6F_5)$_4$]

^1H NMR (C_6D_5Cl, 297K, 400.13 MHz) δ = 7.29 (m, buried with **8**), 7.18 (m, buried with **8**), 6.71 (d, 2H, $^3J_{H,H}$ = 7.8 Hz), 6.08 (brs, 4H), 5.89 (brs, 4H), 2.56 (brs, 6H), 1.07 (s, 18H), 0.98 ppm (s, 3H).

*4.3.4. [(Cp^{t-bu})$_2$Zr(η^2-CH$_2$NMePh)][B(C_6F_5)$_4$] (**8**)*

^1H NMR (C_6D_5Cl, 297K, 400.13 MHz) δ = 7.29 (m, 2H, *meta*-H), 7.22 (m, 2H, *para*-H), 6.83 (brd, 2H, *ortho*-H), 6.77 (ddd, 1H, $H2^u$, $^3J_{H,H}$ = 2.5 Hz), 6.33 (ddd, 1H, $H4^u$, $^3J_{H,H}$ = 2.5 Hz), 6.21 (ddd, 1H, $H3^d$, $^3J_{H,H}$ = 2.5 Hz), 6.04 (ddd, 1H, $H2^u$, $^3J_{H,H}$ = 2.5 Hz), 5.73 (ddd, 1H, $H4^d$, $^3J_{H,H}$ = 2.5 Hz), 5.66 (ddd, 1H, $H1^d$, $^3J_{H,H}$ = 2.5 Hz), 5.39 (ddd, 1H, $H2^d$, $^3J_{H,H}$ = 2.5 Hz), 5.04 (ddd, 1H, $H2^d$, $^3J_{H,H}$ = 2.5 Hz), 3.91 (d, 1H, $ZrCH_2^d$, $^2J_{H,H}$ = 8.7 Hz), 2.86 (s, 3H, NMe), 2.78 (d, 1H, $ZrCH_2^u$, $^2J_{H,H}$ = 8.7 Hz), 0.87 (s, 9H, t-Bu^u), 0.81 ppm (s, 9H, t-Bu^d). $^{13}C\{^1H\}$ NMR (C_6D_5Cl, 297 K, 100.55 MHz) δ = 153.9 (s, *ipso*-C), 143.1 (s, C5-t-Bu^d), 140.9 (s, C5-t-Bu^u), 130.4 (s, *meta*-C), 128.2 (s, *para*-C), 121.2 (s, *ortho*-C), 116.7 (s, $C1^d$), 116.5 (s, $C2^u$), 116.0 (s, $C2^d$), 111.8 (s, $C1^u$), 111.3 (s, $C4^d$), 109.2 (s, $C3^u$), 108.8 (s, $C3^d$), 107.2 (s, $C4^u$), 62.0 (s, $ZrCH_2$), 60.1 (s, NMe), 32.4 (s, CMe t-Bu^d), 32.2 (s, CMe t-Bu^d), 30.0 (s, Me t-Bu^d), 26.1 ppm (s, Me t-Bu^u). ^{19}F NMR (C_6D_5Cl, 297 K, 376.65 MHz) δ = −132.2 (brd, *ortho*-F), −162.6 (t, *para*-F, $^3J_{F,F}$ = 21.3 Hz), −166.5 ppm (m, *meta*-F).

*4.3.5. [(Cp^{n-bu})$_2$Zr(η^2-CH$_2$NMePh)][B(C_6F_5)$_4$] (**9**)*

^1H NMR (C_6D_5Cl, 297 K, 400.13 MHz) δ = 7.28 (m, buried with other aromatic resonances), 7.17 (d, buried with other aromatic resonances, $^3J_{H,H}$ = 7.8 Hz), 7.15 (m, buried with other aromatic resonances), 5.68 (m, buried with other resonances), 5.48 (m, 1H), 5.37 (m, 2H), 5.28 (m, 2H), 5.21 (m, 1H), 4.93 (m, 1H), 2.87 (d, 1H, $^2J_{H,H}$ = 8.4 Hz), 2.51 (s, 3H), 2.22 (d, 1H, $^2J_{H,H}$ = 8.4 Hz), 1.81 (m, buried with other resonances), 1.38 (m, buried with other resonances), 1.31 (m, buried with other resonances), 1.21 (m, buried with other resonances), 1.10 (m, buried with other resonances), 1.03 (m, 4H), 0.99 (m, buried with other resonances), 0.76 ppm (m, 4H). $^{13}C\{^1H\}$ NMR (C_6D_5Cl, 297 K, 100.55 MHz) δ = 155.6 (s), 121.7 (s), 117.9 (s), 117.3 (s), 116.5 (s), 116.1 (s), 115.8 (s), 113.9 (s), 113.2 (s), 112.3 (s), 111.5 (s), 107.4 (s), 105.7 (s), 58.4 (s), 57.2 (s), 45.8 (s), 33.6 (s), 33.4 (s), 33.0 (s), 32.6 (s), 29.5 (s), 29.4 (s), 24.9 (s), 22.6 (s), 22.1 (s), 13.6 (s), 13.4 (s), 13.3 ppm (s). ^{19}F NMR (C_6D_5Cl, 297 K, 376.65 MHz) δ = −132.0 (brd, *ortho*-F), −162.6 (t, *para*-F, $^3J_{F,F}$ = 21.3 Hz), −166.4 ppm (m, *meta*-F).

4.3.6. [(Ind)$_2$ZrMe(NMe$_2$Ph)][B(C_6F_5)$_4$]

^1H NMR (C_6D_5Cl, 297 K, 400.13 MHz) δ = 7.2–6.66 (aromatic resonances buried with **10**), 5.83 (s, buried with **10**), 5.72 (4H), −0.91 (s, 6H), −2.5 ppm (s, 3H).

*4.3.7. [(Ind)$_2$Zr(η^2-CH$_2$NMePh)][B(C_6F_5)$_4$] (**10**)*

^1H NMR (C_6D_5Cl, 297 K, 400.13 MHz) δ = 7.69 (d, 1H, $J_{H,H}$ = 8.4 Hz), 7.65 (d, 1H, $J_{H,H}$ = 8.2 Hz), 7.38 (d, 1H, $J_{H,H}$ = 8.2 Hz), 7.25 (m, buried with other resonances), 7.17 (m, buried with other resonances), 7.08 (m, buried with other resonances), 6.97 (d, 2H, $J_{H,H}$ = 7.6 Hz), 6.90 (m, buried with other resonances), 6.82 (m, 1H), 6.50 (s, 1H), 6.27 (m, buried with other resonances), 6.19 (s, 1H), 6.12 (m, buried with other resonances), 6.07 (s, 1H), 6.00 (m, buried with other resonances), 5.96 (s, 1H), 5.86 (s, 1H), 5.77 (d, 1H, $J_{H,H}$ = 8.2 Hz), 5.65 (s, 1H), 2.36 (s, 3H), 0.52 (d, 1H, $J_{H,H}$ = 7.8 Hz), −0.19 ppm (d, 1H, $J_{H,H}$ = 7.8 Hz). $^{13}C\{^1H\}$ NMR (C_6D_5Cl, 297 K, 100.55 MHz) δ = 152.6 (s), 126.6 (s), 125.5 (s), 124.2 (s), 123.7 (s), 121.9 (s), 120.3 (s), 119.8 (s), 116.2 (s), 114.4 (s), 112.5 (s), 104.3 (s), 103.5 (s), 102.1 (s), 101.9 (s), 101.3 (s), 101.0 (s), 100.6 (s), 100.2 (s), 69.7 (s), 54.9 (s), 45.5 (s), 22.8 ppm (s). ^{19}F NMR (C_6D_5Cl, 297 K, 376.65 MHz) δ = −132.0 (brd, *ortho*-F), −162.6 (t, *para*-F, $^3J_{F,F}$ = 21.3 Hz), −166.4 ppm (m, *meta*-F).

4.4. Partial NMR data for the reaction of $Cp^*_2ZrMe_2$ with 1 equivalent of [HNMePh][B(C_6F_5)$_4$]

^1H NMR (C_6D_6, 297 K, 400.13 MHz) δ = 7.22 (t, 1H, $J_{H,H}$ = 7.8 Hz), 6.80 (m, 2H), 6.62 (d, 2H, $J_{H,H}$ = 7.8 Hz), 2.49 (s, 6H), 1.38 (s, 2.5 H), 1.33 (s, 2H), 1.23 (s, 1.8H), 0.15 (s, CH_4), 0.14 ppm (t, CH_3D).

*4.5. Reaction of **7**, **8** and **10** ion pairs with 2-methyl-1-heptene and NMR data*

Into the glovebox, approximately 10 equivalents of 2-methyl-1-heptene were charged into a micrometric syringe and added to a solution of the azametallacycle in C_6D_5Cl within a J-Young NMR tube. The sample was successively analyzed by NMR spectroscopy after about 10 min.

*4.5.1. **7** + 2-Me-1-heptene*

^1H NMR (C_6D_5Cl, 297 K, 400.13 MHz) δ = 7.25 (m, buried with other aromatic resonances), 7.17 (m, buried with other aromatic resonances), 6.83 (s, 1H), 6.73 (s, 1H), 6.36 (m, 4H), 6.20 (brd, 4H), 5.89 (m, 1H), 5.86 (m, 1H), 5.16 (m, 4H), 5.04 (m, 1H), 3.83 (m, 1H), 3.81 (m, 1H), 3.06 (d, 1H, $J_{H,H}$ = 12.5 Hz), 2.94 (d, 1H, $J_{H,H}$ = 12.5 Hz), 2.64 (s, 3H), 2.63 (s, 3H), 2.58 (d, 1H, $J_{H,H}$ = 12.5 Hz), 2.38 (d, 1H, $J_{H,H}$ = 12.5 Hz), 1.62 (d, 1H), 1.12 (s, 3H), 1.06 (s, 3H), 0.63 (d, 1H, $J_{H,H}$ = 13.8 Hz), 0.43 (s, 6H), 0.10 (s, 3H), 0.09 ppm (s, 3H).

*4.5.2. **10** + 2-Me-1-heptene*

^1H NMR (C_6D_5Cl, 297 K, 400.13 MHz) δ = 7.52 (d, 3H), 7.44 (m, buried with other aromatic resonances), 7.37 (m, buried with other aromatic resonances), 7.28 (m, buried with other aromatic resonances), 7.18 (m, buried with other aromatic resonances), 6.98 (m, buried with other aromatic resonances), 6.9 (m, buried with other aromatic resonances), 6.57 (t, buried with other aromatic resonances), 6.49 (s, buried with other aromatic resonances), 6.41 (t, buried with other aromatic resonances), 6.27 (s, buried with other aromatic resonances), 6.14 (m, buried with other aromatic resonances), 6.07 (s, buried with other aromatic resonances), 5.98 (m, buried with other aromatic resonances), 5.87 (m, 2H), 5.77 (m, 1H), 5.68 (m, 1H), 5.65 (m, 1H), 5.58 (m, 3H), 5.34 (m, 1H), 5.30 (m, buried with other resonances), 5.27 (m, 1H), 4.99 (m, 1H), 3.63 (d, 1H), 3.61 (d, 1H), 2.78 (s, 3H), 2.76 (s, 3H), 2.75 (d, 1H), 2.51 (d, 1H, $J_{H,H}$ = 12.6 Hz), 2.42 (d, 1H, $J_{H,H}$ = 12.6 Hz), 2.36 (s, 3H), 1.06 (s), 0.85 (s, 3H), 0.52 (d, 0.5H, $J_{H,H}$ = 8.2 Hz), −1.21 ppm (d, buried with other resonances, $J_{H,H}$ = 14.2 Hz). $^{13}C\{^1H\}$ NMR (C_6D_5Cl, 297 K, 100.55 MHz) δ = 152.8 (s), 148.6 (s), 147.8 (s), 145.7 (s), 132.2 (s), 132.1 (s), 128.7 (s), 127.0 (s), 126.9 (s), 126.8 (s), 126.7 (s), 126.5 (s), 126.3 (s), 125.3 (s), 125.2 (s), 124.9 (s), 124.7 (s), 124.6 (s), 124.4 (s), 124.2 (s), 124.0 (s), 123.8 (s), 123.7 (s), 123.5 (s), 122.8 (s), 121.5 (s), 119.9 (s), 117.4 (s), 117.3 (s), 117.2 (s), 116.3 (s), 116.2 (s), 114.6 (s), 112.7 (s), 109.9 (s), 107.4 (s), 106.7 (s), 106.2 (s), 106.1 (s), 105.6 (s), 105.4 (s), 104.8 (s), 104.2 (s), 103.9 (s), 102.2 (s), 101.3 (s), 100.4 (s), 99.9 (s), 70.2 (s), 69.8 (s), 69.1 (s), 56.3 (s), 55.7 (s), 46.6 (s), 46.4 (s), 42.8 (s), 42.6 (s), 37.9 (s), 32.7 (s), 32.5 (s), 32.2 (s), 30.2 (s), 29.8 (s), 27.9 (s), 27.4 (s), 25.6 (s), 24.1 (s), 23.6 (s), 22.7 (s), 22.2 (s), 14.1 ppm (s).

Acknowledgments

This work was supported by grants from the Ministero dell'Istruzione, dell'Università e della Ricerca through the PRIN 2009 LR88XR program.

Appendix. Supplementary material

Supplementary material associated with this article can be found, in the online version, at doi:10.1016/j.jorganchem.2012.02.011.

References

[1] H.H. Brintzinger, D. Fischer, R. Mulhaüpt, B. Rieger, R. Waymouth, Angew. Chem. 34 (1995) 1143–1170.
[2] C.E. Zachmanoglou, A. Docrat, B.M. Bridgewater, G. Parkin, C.G. Brandow, J.E. Bercaw, C.N. Jardine, M. Lyall, J.C. Green, J.B. Keister, J. Am. Chem. Soc. 124 (2002) 9525–9546.
[3] L. Resconi, J.C. Chadwick, L. Cavallo, in: R.H. Crabtree, D.M.P. Mingos (Eds.), Comprehensive Organometallic Chemistry III, vol. 4, ELSEVIER, Oxford, 2007 (Chapter 9).
[4] V.L. Cruz, J. Ramos, S. Martinez, A. Muñoz-Escalona, J. Martinez-Salazar, Organometallics 24 (2005) 5095–5102.
[5] P.C. Möhring, N.J. Coville, J. Organomet. Chem. 479 (1994) 1–29.
[6] P.C. Möhring, N.J. Coville, Coord. Chem. Rev. 250 (2006) 18–35.
[7] T. Piel, T. Saarinen, B. Löfgren, E. Kokko, J. Maaranen, P. Pitkänen, Macromol. Chem. Phys. 208 (2007) 851–861.
[8] T.A. Manz, S. Sharma, K. Phomphrai, K.A. Novstrup, A.E. Fenwick, P.E. Fanwick, G.A. Medvedev, M.M. Abu-Omar, W.N. Delgass, K.T. Thomson, J.M. Caruthers, Organometallics 27 (2008) 5504–5520.
[9] A. Macchioni, Chem. Rev. 105 (2005) 2039–2074.
[10] M. Bochmann, Organometallics 29 (2010) 4711–4740.
[11] E.Y.X. Chen, T.J. Marks, Chem. Rev. 100 (2000) 1391–1434.
[12] C.N. Rowley, T.K. Woo, Organometallics 30 (2011) 2071–2074.
[13] H.W. Turner, Eur. Pat. Appl. 0277004 (1998).
[14] $pK_B = 8.85$ for N, N dimethylanilineR.C. West (Ed.), CRC Handbook of Chemistry and Physics, 67th ed. CRC Press, Boca Raton, 1987 section D-161.
[15] A.D. Horton, A.G. Orpen, Organometallics 10 (1991) 3910–3918.
[16] F. Schaper, A. Geyer, H.H. Brintzinger, Organometallics 21 (2002) 473–483.
[17] P.A. Wilson, J.A. Wright, V.S. Oganesyan, S.J. Lancaster, M. Bochmann, Organometallics 27 (2008) 6371–6374.
[18] L. Rocchigiani, C. Zuccaccia, D. Zuccaccia, A. Macchioni, Chem. Eur. J. 14 (2008) 6589–6592.
[19] L. Rocchigiani, G. Bellachioma, G. Ciancaleoni, A. Macchioni, D. Zuccaccia, C. Zuccaccia, Organometallics 30 (2011) 100–114.
[20] H.W. Turner, G.G. Hlatky, R.R. Eckman U.S. Patent 5,198,401 (1993).
[21] O. Wrobel, F. Schaper, U. Weiser, H. Gregorius, H.H. Brintzinger, Organometallics 22 (2003) 1320–1325.
[22] L. Rocchigiani, A. Macchioni, C. Zuccaccia, submitted for publication.
[23] L. Rocchigiani, G. Ciancaleoni, C. Zuccaccia, A. Macchioni, Angew. Chem. Int. Ed. 50 (2011) 11752–11755.
[24] F. Wu, A.K. Dash, R.F. Jordan, J. Am. Chem. Soc. 126 (2004) 15360–15361.
[25] I.G. Rios, E. Novarino, S. van der Veer, B. Hessen, M.W. Bouwkamp, J. Am. Chem. Soc. 131 (2009) 16658–16659.
[26] C. Janiak, K.C.H. Lange, U. Versteeg, D. Lentz, P.H.M. Budzelaar, Chem. Ber. 129 (1996) 1517–1529.
[27] U. Wieser, F. Schaper, H.H. Brintzinger, N.I. Mäkelä, H.R. Knuuttila, M. Leskelä, Organometallics 21 (2002) 541–545.
[28] U. Wieser, D. Babuskin, H.H. Brintzinger, Organometallics 21 (2002) 920–923.
[29] A. Macchioni, Eur. J. Inorg. Chem. (2003) 195–205.
[30] G. Bellachioma, G. Cardaci, V. Gramlich, A. Macchioni, M. Valentini, C. Zuccaccia, Organometallics 17 (1998) 5025–5030.
[31] R. Romeo, L. Fenech, L.M. Scolaro, A. Albinati, A. Macchioni, C. Zuccaccia, Inorg. Chem. 40 (2001) 3293–3302.
[32] G. Bellachioma, B. Binotti, G. Cardaci, C. Carfagna, A. Macchioni, S. Sabatini, C. Zuccaccia, Inorg. Chim. Acta 330 (2002) 44–51.
[33] B. Binotti, G. Bellachioma, G. Cardaci, A. Macchioni, C. Zuccaccia, E. Foresti, P. Sabatino, Organometallics 21 (2002) 346–354.
[34] A. Macchioni, A. Magistrato, I. Orabona, F. Ruffo, U. Rothlisberger, C. Zuccaccia, New J. Chem. 27 (2003) 455–458.
[35] D. Zuccaccia, G. Bellachioma, G. Cardaci, G. Ciancaleoni, C. Zuccaccia, E. Clot, A. Macchioni, Organometallics 26 (2007) 3930–3946.
[36] D. Zuccaccia, L. Belpassi, F. Tarantelli, A. Macchioni, J. Am. Chem. Soc. 131 (2009) 3170–3171.
[37] C. Zuccaccia, N.G. Stahl, A. Macchioni, M.-C. Chen, J.A. Roberts, T.J. Marks, J. Am. Chem. Soc. 126 (2004) 1448–1464.
[38] K. Plössl, J.R. Norton, J.G. Davidson, E.K. Barefield, Organometallics 11 (1992) 534–539.
[39] J. Jeener, B.H. Meier, P. Bachmann, R.R. Ernst, J. Chem. Phys. 71 (1979) 4546–4553.
[40] R. Wagner, S. Berger, J. Magn. Reson. A 123 (1996) 119–121.
[41] B. Lix, F.D. Sönnichsen, B.D. Sykes, J. Magn. Reson. A 123 (1996) 119–121.
[42] E. Samuel, M.D. Rausch, J. Am. Chem. Soc. 95 (1973) 6263–6267.